

Experimental study of the influence of periodic boundary conditions: Effects of finite size and faster cooling rates on dissimilar polymer-polymer interfaces

Roman R. Baglay and Connie B. Roth*

Department of Physics, Emory University, Atlanta, Georgia 30322 USA

*To whom correspondence should be addressed: cbroth@emory.edu

Submitted to *ACS Macro Letters* on July 3, 2017;

Accepted August 4, 2017; Published August 7, 2017

ABSTRACT: Building on our recent work that mapped the profile in local glass transition temperature $T_g(z)$ across a single polystyrene (PS) / poly(*n*-butyl methacrylate) (PnBMA) interface, we explore the impact of limiting domain size and increasing cooling rate. This study is motivated by traditional computational approaches employed to overcome computer-power limitations, extrapolating short time scales and using periodic boundary conditions that introduce repeating interfaces. Using a localized fluorescence method, we find addition of a second PS/PnBMA interface perturbs the local PS $T_g(z)$ at a distance of $z = 100$ nm from the first interface when the second interface approaches a distance closer than 300 nm. The local $T_g(z)$ profile across a finite PS domain size of 300 nm for a range of cooling rates shows that limiting domain size and increasing cooling rate (faster timescales) diminishes and truncates the broad asymmetric $T_g(z)$ profile, weakening the confinement effect for dissimilar polymer-polymer interfaces, consistent with previous studies on single-layer polymer films.

Studies of glass transition perturbations due to dissimilar polymer-polymer interfaces have recently gained interest.¹⁻²⁰ Experimentally, these polymer-polymer interfaces show dynamical perturbations persisting to larger distances from the interface than for a polymer-free surface.^{9,10} Efforts to model such long-ranged effects to slow glass transition dynamics are hampered by typical limitations of computational power. Traditionally these limitations are bypassed by employing periodic boundary conditions²¹ and extrapolating the temperature dependence of simulated short time scales down to lower temperatures.^{1,22-24} Here we are interested in experimentally exploring what effects these traditional computational strategies have on the observed length-scales of dissimilar polymer-polymer interfaces. Previous studies

on single-layer polymer films have shown that limiting the system size can lead to a reduction in the gradient in dynamics near a free surface resulting in a more homogeneous profile,²⁵ and that the use of faster cooling rates²⁶ or focus on faster time scales²⁷ can truncate the magnitude and length scales of confinement effects.

We build on our recent work employing a localized fluorescence method to map out the full profile in local glass transition temperature $T_g(z)$ across a polystyrene (PS) / poly(*n*-butyl methacrylate) (PnBMA) interface.⁹ For this semi-infinite bilayer system, the dynamical perturbation is free to extend as far as needed into the material before recovering the bulk T_g value on either side of the interface (PS $T_g^{\text{bulk}} = 101$ °C, PnBMA $T_g^{\text{bulk}} = 21$ °C). We have found this perturbation distance from the interface to be dependent on whether the polymer forms the high- T_g glassy component, with dynamical perturbations persisting for 225-250 nm before bulk T_g is recovered, or the low- T_g rubbery component, with perturbations persisting for 100-125 nm.¹⁰ These broad and asymmetric $T_g(z)$ profiles are common across a number of dissimilar polymer-polymer interfaces and are observed to be much larger and uncorrelated with the 5-7 nm interfacial width in equilibrium composition profile.⁹ We have also demonstrated that the extent of chain interpenetration across the dissimilar polymer-polymer interface is important to coupling the dynamics between the two polymers and creating the broad and asymmetric $T_g(z)$ profile observed when the dissimilar polymer-polymer interface is annealed to equilibrium.¹⁰

In the present study, we explore the effect of adding a second PS/PnBMA interface, creating a PS domain of finite size, to the local $T_g(z)$. Molecular dynamics (MD) simulations of a single dissimilar polymer-polymer interface that employ periodic boundary conditions wrap the system in all three dimensions, which extends the system size in two dimensions, but inherently introduces additional perturbative interfaces and limits the domain size in the other dimension.¹ Such simulations are good models of extruded alternating nanolayered systems¹⁴⁻¹⁷ as intended, or perhaps lamellae forming block copolymers, but we believe they are distinctly different than our previous experiments on semi-infinite bilayers where the interfacial perturbations can propagate unrestricted. Here we explore the difference between such systems, finding that the addition of a second PS/PnBMA interface already perturbs the local $T_g(z)$ value at $z = 100$ nm from the first PS/PnBMA interface when the domain size is restricted to below ≈ 400 nm in size. We map out the local $T_g(z)$ profile for a finite PS domain size of 300 nm, observing that bulk T_g of PS is not recovered at its center. In addition, we increase the cooling rate and find that the

$T_g(z)$ profile becomes muted. Although we are experimentally limited to cooling rates between 1-15 K/min, we observed trends consistent with previous experiments^{26,28} suggesting simulations focused on faster time scales would observe weakened confinement effects with shorter length scales.

Following our previous works,^{9,10} single layer films of neat PS ($M_w = 1920$ kg/mol, $M_w/M_n = 1.26$, Pressure Chemical), pyrene-labeled PS ($M_w = 672$ kg/mol, $M_w/M_n = 1.3$, free-radically polymerized with 1.4 mol% pyrene content⁹), and PnBMA ($M_w = 1210$ kg/mol, $M_w/M_n = 1.7$, free-radically polymerized⁹) were spin-coated from toluene solutions onto freshly-cleaved mica and independently annealed overnight under vacuum at 120 °C for PS or 80 °C for PnBMA layers. Multilayer stacks, as depicted in Figure 1, were then assembled by successively floating layers of desired thickness (measured by ellipsometry Woollam M-2000) atop each other placing the 11-12 nm PS-Py labeled layer at a distance z from the bottom PS/PnBMA interface and a distance y from the second, top PS/PnBMA interface. The finite PS domain size is determined from the sum of the PS layers ($z + \text{PS-Py} + y$). As described previously,^{9,10} the multilayer stack is then carefully annealed at 120 °C for 20 min to ensure the PS/PnBMA dissimilar polymer-polymer interfaces are annealed to equilibrium, while consolidating the PS/PS-Py interfaces into a single material, but keeping the PS-Py labeled layer localized. Fluorescence intensity was then collected on cooling using a Photon Technology International QuantaMaster spectrofluorometer (excitation at 330 nm, emission intensity monitored at 379 nm, band-passes of 5-6 nm) with the samples mounted in a Peltier-cooled Instec TS62 temperature stage with dry nitrogen flowing at 1.7 L/min directly onto the sample cover slip to avoid condensation below room temperature. At the end of the run, all samples were reheated to the initial starting temperature to ensure the same fluorescence intensity was recovered. Intensity data was collected for 3 s every 27 s on cooling at 1 K/min or every 7 s cooling at 10 and 15 K/min. The local T_g of the PS-Py layer is manifested as the intersection of linear fits to the liquid and glassy regimes by maximizing the R^2 on each side of the transition. The largest uncertainty in the measured T_g values comes from sample-to-sample variability, which we find to be ± 2 °C from an average of multiple samples (typically smaller than the symbol size); the uncertainty in T_g from the fitting is much less.¹⁰

Figure 1 illustrates the different samples we are comparing in this study by plotting the fluorescence emission intensity measured on cooling at 1 K/min for a series of different representative samples where the local $T_g(z,y)$ measured by the pyrene-labeled layer depends on

its distance from the two PS/PnBMA interfaces (z is the distance from the bottom interface and y the distance from the top interface). The top two curves confirm the results from our previous work:⁹ far from either interface the bulk T_g value of PS is recovered $T_g(z = 356 \text{ nm}, y > 450 \text{ nm}) = 100 \pm 2 \text{ }^\circ\text{C}$, and when one interface is approached, the local T_g becomes significantly reduced $T_g(z = 100 \text{ nm}, y > 450 \text{ nm}) = 65 \pm 2 \text{ }^\circ\text{C}$. The lower two curves address the question of when the presence of a second PS/PnBMA interface affects these results. From the data we can see that this occurs when the second interface is somewhere between 260-301 nm: $T_g(z = 100 \text{ nm}, y = 301 \text{ nm}) = 66 \pm 2 \text{ }^\circ\text{C}$ is consistent with the data when the second y -interface is far away, while $T_g(z = 100 \text{ nm}, y = 260 \text{ nm}) = 63 \pm 2 \text{ }^\circ\text{C}$ is now further reduced by the presence of this second y -interface. This distance of $\sim 275 \text{ nm}$ is approximately the distance at which bulk T_g of PS was recovered from the single PS/PnBMA interface in our previous study⁹ (see inset of Fig. 2).

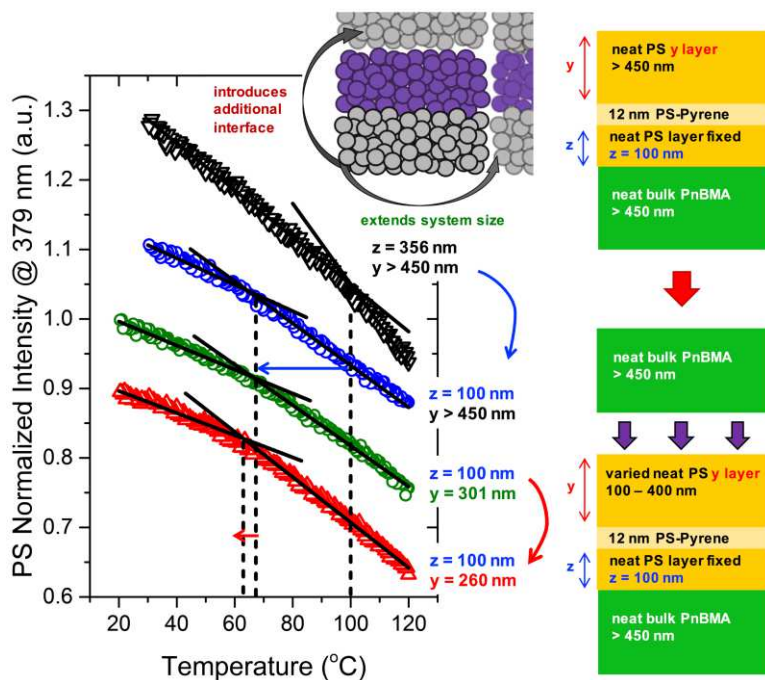


Figure 1. Temperature-dependent fluorescence intensity collected on cooling at 1 K/min to identify $T_g(z,y)$ of a 12-nm pyrene-labeled-PS layer located a distance z from the bottom PS/PnBMA interface and a distance y from the top PS/PnBMA interface.

To more precisely identify when the presence of this second y -interface begins to further perturb the local dynamics, we measured a series of different samples all at a fixed distance $z = 100 \text{ nm}$ from the bottom PS/PnBMA interface with varying distance y from the top PS/PnBMA

interface, as plotted in Figure 2. When the top y -interface is far away ($y > 300$ nm), the local $T_g(z = 100 \text{ nm}, y > 300 \text{ nm}) = 66 \pm 1.6 \text{ }^\circ\text{C}$ (based on an average of 5 samples) are consistent with the range of local $T_g(z = 100 \text{ nm}) = 64\text{--}69 \text{ }^\circ\text{C}$ (represented by the shaded horizontal-blue bar) measured in our previous study with only a single interface,⁹ as depicted in the inset of Fig. 2. Note that this is significantly reduced from the bulk- T_g value of PS = $101 \pm 2 \text{ }^\circ\text{C}$ indicated at the top of the figure. With decreasing y -distance from the second (top) interface, we observe a further decrease in local $T_g(z,y)$ due to the presence of the second interface when $y \leq 290 \pm 10$ nm, a quantitative estimate based on where a linear extrapolation of the data for $y < 275$ nm intersects with the shaded horizontal-blue bar. These data demonstrate that deviations to the local dynamics from finite domain sizes occur at quite large values for these heterogeneous polymer-polymer systems.

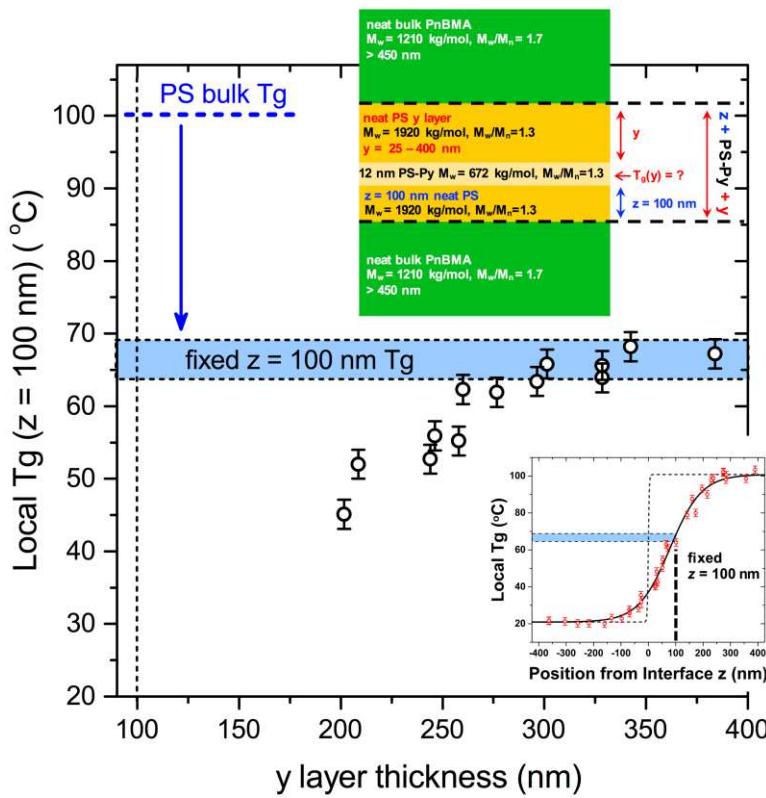


Figure 2. Local $T_g(z,y)$ at a fixed distance $z = 100 \text{ nm}$ from the bottom PS/PnBMA interface as a function of y -distance from the top PS/PnBMA interface. Horizontal-blue bar indicates local PS $T_g(z = 100 \text{ nm}) = 64\text{--}69 \text{ }^\circ\text{C}$ depression due to a single PS/PnBMA interface identified in Ref. 9 (shown in inset). Presence of second PS/PnBMA interface leads to further $T_g(z,y)$ decrease

below $y = 290 \pm 10$ nm.

We now probe what the local $T_g(z,y)$ profile is in such a domain of finite size. We chose to focus on a total domain size $z + y = 300$ nm because, based on the data shown in Fig. 2, such a domain size should be small enough to exhibit substantial perturbations to the local $T_g(z,y)$ profile relative to that for a single interface, while still remaining large enough such that the two PS/PnBMA interfaces, separated by 300 nm, should not feel each other. This means that the local T_g reductions at each of the PS/PnBMA interfaces should be effectively decoupled and match that of the T_g reduction near a single PS/PnBMA interface. Figure 3 plots the local $T_g(z,y)$ profile across a 300-nm PS domain as a function of distance z from the first PS/PnBMA interface. Data were measured for a series of different samples with z varying from 25-150 nm (solid symbols), while the y -layer was correspondingly varied to maintain a total domain size of $z + y = 300$ nm. By symmetry, the $T_g(z,y)$ profile was extended to $z = 175-275$ nm (open symbols) by mirroring the data about the midpoint of the domain. The open blue symbol at the PS/PnBMA interface was taken from our previous work,⁹ where the local $T_g(z = 0)$ was found to be 37 °C at the (single) PS/PnBMA interface. The curves through the data are simply a guide to the eye, but highlight how this local $T_g(z,y)$ profile within a finite domain size is flattened and truncated relative to that found for a single PS/PnBMA interface (inset of Fig. 2) where the semi-infinite PS domain allowed the interfacial perturbation to propagate as far as necessary for the dynamics to recover bulk T_g . This experimental $T_g(z,y)$ profile is qualitatively similar to the local mobility profile predicted by Tito et al.² for slabs of rubbery/glassy/rubberly material where they also find that the interfacial perturbation to the local dynamics persists deeper into the material within the glassy domain.

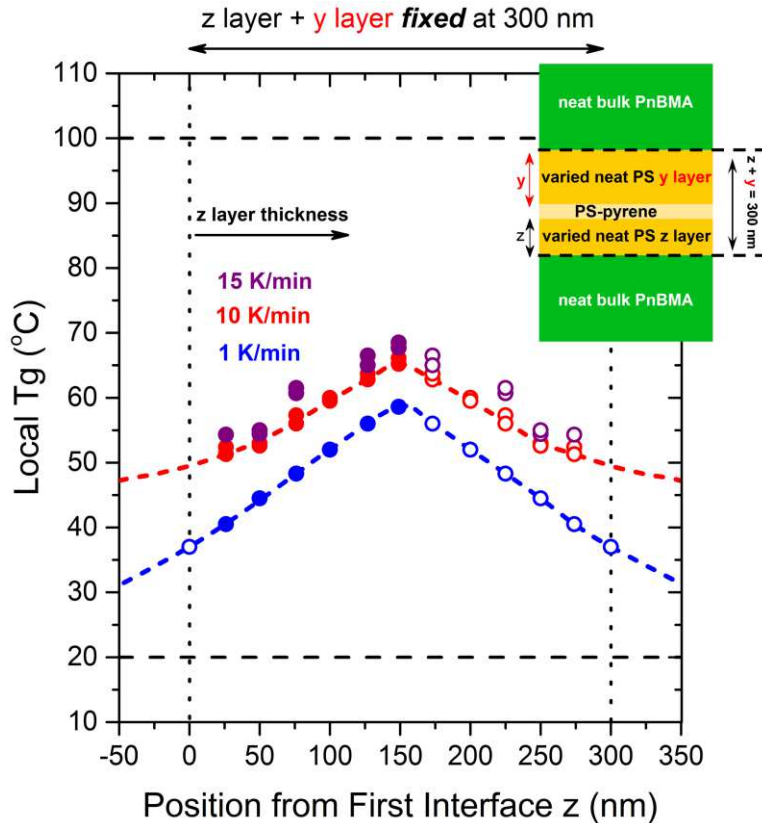


Figure 3. Local $T_g(z,y)$ profile across a 300-nm PS domain sandwiched between two semi-infinite PnBMA layers measured at cooling rates of 1, 10, 15 K/min.

Figure 3 also explores the impact of increasing cooling rate on the measured $T_g(z,y)$ profile, where data collected at cooling rates of 10 and 15 K/min are included. Though we are experimentally limited to a small window of cooling rates, we find that the cooling-rate dependence shown in Fig. 3 is empirically equivalent to the film-thickness dependent $T_g(h)$ cooling-rate data reported previously for single-layer supported PS films,^{26,28,29} probing the same underlying physics as fragility.²⁹ Fakhraai and Forrest originally demonstrated using ellipsometry that increasing the cooling rate from 1-130 K/min resulted in a diminished $T_g(h)$ reduction with a weakened confinement effect.²⁶ These studies find that the largest change in $T_g(h)$ occurs at smaller cooling rates.^{28,29} For example, Glor and Fakhraai²⁸ see an approximate 10 K increase in $T_g(h)$ for a 10-nm thick film when increasing the cooling rate from 1 to 7 K/min. Similarly, we observe a roughly 10 K increase in local $T_g(z,y)$ near the PS/PnBMA interface when increasing the cooling rate from 1 to 10 K/min. Thus, consistent with these previous works, we also observe a diminished and weakened confinement effect with increased cooling

rate in these heterogeneous polymer-polymer systems.

Interestingly we do not observe that PS bulk T_g is recovered at the center of this 300 nm domain. Previous work comparing pyrene-fluorescence to ellipsometry in single-layer PS films³⁰ finds that pyrene-fluorescence only identifies a single T_g value, biased towards the low end of the temperature range, even when the ellipsometry data demonstrates a broad transition in thermal expansion coefficient. This suggests there could be a wider distribution of relaxation times present at a given (z,y) position, but pyrene-fluorescence may only be sensitive to what corresponds to a faster subset of such a distribution. At present this pyrene-fluorescence method is the only experimental technique able to provide such local, depth-dependent information. Previous localized dielectric methods^{31,32} have been limited to comparatively fast time scales (>1 Hz) at higher temperatures where such confinement effects would be expected to be weaker. Thus, new experimental techniques with depth-dependent, long-time (sub-Hz) resolution are needed.

These results of adding a second interface and increasing the cooling rate suggest that if computational studies, necessarily at fast time scales, are going to study such effects with periodic boundary conditions that create finite domain sizes, one would expect to observe shortened length scales and weaker confinement effects. Our study has only focused on limiting the PS domain size (similar to the work of Tito et al.²); we do not address what impact limiting the domain size of PnBMA would have that is relevant for nanolayered systems with alternating polymer layers^{1,14-17} or block-copolymer self-assembled lamellae systems.¹⁸⁻²⁰ Regardless, the results presented here provide important information about the relevant length scales within materials with dissimilar polymer-polymer interfaces, for picking system sizes where the presence of additional interfaces could be inadvertently affecting the local dynamics. Although the present study does not address the underlying cause for the long length scales observed experimentally, it does provide some reasoning for why computer simulations would see smaller length scales. Experimental efforts are underway to address the underlying cause of the long length scales in the systems.¹⁰ We believe experiments such as the ones in this study of local properties near dissimilar polymer-polymer interfaces could eventually provide some predictive power to infer the macroscopic properties of heterogeneous polymer materials with different morphologies.

Acknowledgements. The authors gratefully acknowledge support from the National Science Foundation Polymers program (DMR-1151646 and DMR-1709132) and Emory University. We are also thank Gino Elia for help with some early measurements.

References:

- (1) Lang, R. J.; Merling, W. L.; Simmons, D. S. Combined Dependence of Nanoconfined T_g on Interfacial Energy and Softness of Confinement. *ACS Macro Lett.* **2014**, *3*, 758–762.
- (2) Tito, N. B.; Lipson, J. E. G.; Milner, S. T. Lattice Model of Mobility at Interfaces: Free Surfaces, Substrates, and Bilayers. *Soft Matter* **2013**, *9*, 9403–9413.
- (3) Roth, C. B.; McNerny, K. L.; Jager, W. F.; Torkelson, J. M. Eliminating the Enhanced Mobility at the Free Surface of Polystyrene: Fluorescence Studies of the Glass Transition Temperature in Thin Bilayer Films of Immiscible Polymers. *Macromolecules* **2007**, *40*, 2568–2574.
- (4) Roth, C. B.; Torkelson, J. M. Selectively Probing the Glass Transition Temperature in Multilayer Polymer Films: Equivalence of Block Copolymers and Multilayer Films of Different Homopolymers. *Macromolecules* **2007**, *40*, 3328–3336.
- (5) Koh, Y. P.; Simon, S. L. Structural Relaxation of Stacked Ultrathin Polystyrene Films. *J Polym Sci, Part B: Polym Phys* **2008**, *46*, 2741–2753.
- (6) Rharbi, Y. Reduction of the Glass Transition Temperature of Confined Polystyrene Nanoparticles in Nanoblends. *Phys Rev E* **2008**, *77*, 031806.
- (7) Robertson, C. G.; Hogan, T. E.; Rackaitis, M.; Puskas, J. E.; Wang, X. Effect of Nanoscale Confinement on Glass Transition of Polystyrene Domains From Self-Assembly of Block Copolymers. *J Chem Phys* **2010**, *132*, 104904.
- (8) Rauscher, P. M.; Pye, J. E.; Baglay, R. R.; Roth, C. B. Effect of Adjacent Rubbery Layers on the Physical Aging of Glassy Polymers. *Macromolecules* **2013**, *46*, 9806–9817.
- (9) Baglay, R. R.; Roth, C. B. Communication: Experimentally Determined Profile of Local Glass Transition Temperature Across a Glassy-Rubbery Polymer Interface with a T_g Difference of 80 K. *J Chem Phys* **2015**, *143*, 111101.
- (10) Baglay, R. R.; Roth, C. B. Local Glass Transition Temperature $T_g(z)$ of Polystyrene Next to Different Polymers: Hard vs. Soft Confinement. *J Chem Phys* **2017**, *146*, 203307.
- (11) Yoon, H.; McKenna, G. B. Substrate Effects on Glass Transition and Free Surface Viscoelasticity of Ultrathin Polystyrene Films. *Macromolecules* **2014**, *47*, 8808–8818.
- (12) Evans, C. M.; Kim, S.; Roth, C. B.; Priestley, R. D.; Broadbelt, L. J.; Torkelson, J. M. Role of Neighboring Domains in Determining the Magnitude and Direction of T_g -Confinement Effects in Binary, Immiscible Polymer Systems. *Polymer* **2015**, *80*, 180–187.

(13) Evans, C. M.; Narayanan, S.; Jiang, Z.; Torkelson, J. M. Modulus, Confinement, and Temperature Effects on Surface Capillary Wave Dynamics in Bilayer Polymer Films Near the Glass Transition. *Phys Rev Lett* **2012**, *109*, 038302.

(14) Liu, R. Y. F.; Jin, Y.; Hiltner, A.; Baer, E. Probing Nanoscale Polymer Interactions by Forced-Assembly. *Macromol Rapid Comm* **2003**, *24*, 943–948.

(15) Liu, R. Y. F.; Bernal-Lara, T. E.; Hiltner, A.; Baer, E. Polymer Interphase Materials by Forced Assembly. *Macromolecules* **2005**, *38*, 4819–4827.

(16) Arabeche, K.; Delbreilh, L.; Adhikari, R.; Michler, G. H.; Hiltner, A.; Baer, E.; Saiter, J.-M. Study of the Cooperativity at the Glass Transition Temperature in PC/PMMA Multilayered Films: Influence of Thickness Reduction From Macro- to Nanoscale. *Polymer* **2012**, *53*, 1355–1361.

(17) Casalini, R.; Zhu, L.; Baer, E.; Roland, C. M. Segmental Dynamics and the Correlation Length in Nanoconfined PMMA. *Polymer* **2016**, *88*, 133–136.

(18) Sethuraman, V.; Pryamitsyn, V.; Ganesan, V. Influence of Molecular Weight and Degree of Segregation on Local Segmental Dynamics of Ordered Block Copolymers. *J Polym Sci, Part B: Polym Phys* **2016**, *54*, 859–864.

(19) Sethuraman, V.; Pryamitsyn, V.; Ganesan, V. Normal Modes and Dielectric Spectra of Diblock Copolymers in Lamellar Phases. *Macromolecules* **2016**, *49*, 2821–2831.

(20) Sethuraman, V.; Ganesan, V. Segmental Dynamics in Lamellar Phases of Tapered Copolymers. *Soft Matter* **2016**, *12*, 7818–7823.

(21) Baschnagel, J.; Varnik, F. Computer Simulations of Supercooled Polymer Melts in the Bulk and in-Confinement Geometry. *J Phys: Condens Matter* **2005**, *17*, R851–R953.

(22) Mangalara, J. H.; Mackura, M. E.; Marvin, M. D.; Simmons, D. S. The Relationship Between Dynamic and Pseudo-Thermodynamic Measures of the Glass Transition Temperature in Nanostructured Materials. *J Chem Phys* **2017**, *146*, 203316.

(23) Hanakata, P. Z.; Douglas, J. F.; Starr, F. W. Interfacial Mobility Scale Determines the Scale of Collective Motion and Relaxation Rate in Polymer Films. *Nat Commun* **2014**, *5*, 4163.

(24) Hanakata, P. Z.; Pazmiño Betancourt, B. A.; Douglas, J. F.; Starr, F. W. A Unifying Framework to Quantify the Effects of Substrate Interactions, Stiffness, and Roughness on the Dynamics of Thin Supported Polymer Films. *J Chem Phys* **2015**, *142*, 234907.

(25) Ellison, C. J.; Torkelson, J. M. The Distribution of Glass-Transition Temperatures in Nanoscopically Confined Glass Formers. *Nature Materials* **2003**, *2*, 695–700.

(26) Fakhraai, Z.; Forrest, J. A. Probing Slow Dynamics in Supported Thin Polymer Films. *Phys Rev Lett* **2005**, *95*, 025701.

(27) Fukao, K.; Miyamoto, Y. Slow Dynamics Near Glass Transitions in Thin Polymer Films. *Phys Rev E* **2001**, *64*, 011803.

(28) Glor, E. C.; Fakhraai, Z. Facilitation of Interfacial Dynamics in Entangled Polymer Films. *J Chem Phys* **2014**, *141*, 194505.

(29) Lan, T.; Torkelson, J. M. Fragility-Confinement Effects: Apparent Universality as a

Function of Scaled Thickness in Films of Freely Deposited, Linear Polymer and Its Absence in Densely Grafted Brushes. *Macromolecules* **2016**, *49*, 1331–1343.

(30) Kim, S.; Hewlett, S. A.; Roth, C. B.; Torkelson, J. M. Confinement Effects on Glass Transition Temperature, Transition Breadth, and Expansivity: Comparison of Ellipsometry and Fluorescence Measurements on Polystyrene Films. *Eur Phys J E* **2009**, *30*, 83–92.

(31) Rotella, C.; Napolitano, S.; De Cremer, L.; Koeckelberghs, G.; Wubbenhorst, M. Distribution of Segmental Mobility in Ultrathin Polymer Films. *Macromolecules* **2010**, *43*, 8686–8691.

(32) Fukao, K.; Takaki, H.; Hayashi, T. Heterogeneous Dynamics of Multilayered Thin Polymer Films. In *Dynamics in Geometrical Confinement*; Kremer, F., Ed.; Advances in Dielectrics; Springer International Publishing: Cham Heidelberg, 2014; pp. 179–212.

TOC Graphic

